Catalysis Today 151 (2010) 53–57

Contents lists available at ScienceDirect

Catalysis Today

journal homepage: www.elsevier.com/locate/cattod

Visible-light photocatalytic hydrogen production from ethanol–water mixtures using a Pt–CdS–TiO_2 photocatalyst

Nikoleta Strataki[a], Maria Antoniadou[a], Vassilios Dracopoulos[b], Panagiotis Lianos[a,*]

[a] Engineering Science Dept., University of Patras, GR-26500 Patras, Greece
[b] Foundation of Research and Technology Hellas-Institute of Chemical Engineering and High Temperature Chemical Processes (FORTH/ICE-HT), P.O. Box 1414, GR-26504 Patras, Greece

ARTICLE INFO

Keywords:
Hydrogen production
Photocatalytic
Cadmium sulfide
Titania

ABSTRACT

Hydrogen was produced by photocatalytic treatment of water–ethanol mixtures. Nanocrystalline titania films, made of commercial Degussa P25, were deposited on transparent conductive glass slides (electrodes) bearing a fluorine-doped tin oxide (FTO) layer. The titania film covered 2/3 of the area of the electrode. On the remaining 1/3 of the area, Pt was deposited by solution casting. Finally, CdS was deposited on nanocrystalline titania. This configuration, which, in reality acts as a photoelectrochemical cell with short-circuited anode and cathode, was used to photocatalytically treat water–ethanol mixtures and produce hydrogen under Visible-light irradiation. The conductive substrate was necessary to drain photogenerated electrons and channel them to the Pt-covered area where reduction interactions took place. The CdS/n-TiO_2 was necessary for Visible-light response. Spatial separation of Pt from CdS/n-TiO_2 was chosen because the mixture of all three agents, i.e., titania, CdS and Pt was found incompatible. In the absence of ethanol, hydrogen production was very slow. In the presence of ethanol, the quantity of hydrogen increased by about an order of magnitude.

1. Introduction

Photocatalytic oxidation of water-soluble organic substances that leads to hydrogen production is an interesting procedure, which can be used for water treatment with energy applications. When a semiconductor photocatalyst, in contact with water and the dissolved organic substance, is excited by absorption of light, an electron–hole pair is generated. Holes interact and oxidize the organic substance or water itself, either directly or through $OH^{\bullet}$ radical intermediates. Oxidation liberates hydrogen ions [1–4], which are reduced by excited electrons and produce molecular hydrogen. If a pure photocatalyst is used, the quantity of hydrogen produced is very small and hardly detectable. This is, due to electron–hole recombination or other chemical reactions, for example, excited electron scavenging by dissolved molecular oxygen, which compete with molecular hydrogen production and they prevail. When, however, noble metal nanoparticles [5,6], i.e., metals with high work function, are deposited on the photocatalyst, tiny Schottky barriers are formed, which lead to electron trapping. In that case, hydrogen evolution is not only easily detected but it becomes impressive indeed. We have recently studied this process, synthesized various photocatalysts and designed immobilized photocatalyst configurations for the photocatalytic hydrogen production from biomass-derived substances [7,8] as well as some water pollutants. The results were interesting and encouraging.

The typical problem faced with TiO_2 photocatalyst, i.e., its absorption only in the UV part of the solar spectrum, is also faced in the case of photocatalytic (PC) hydrogen production. For this reason, we have tried to photosensitize n-TiO_2 by using various substances. It is very hard to find organic molecular photosensitizers that work in an aqueous environment. Titania photosensitization by molecular photosensitizers is mostly celebrated in the case of organic solar cells. However, in that case, the environment is strictly non-aqueous. Some low band-gap semiconductors, like CdS, do act as photocatalysts for hydrogen production in aqueous media [9,10]. It can also be combined with titania for the same purpose [11]. Even though, such materials are vulnerable to oxidation themselves, their functionality can be preserved when the oxidative holes are efficiently scavenged and eliminated. Thus in the present work we employed CdS, which was deposited on n-TiO_2 by repetitive adsorption of the constituent ionic species from aqueous solutions. CdS acts as photosensitizer under Visible-light irradiation. In the course of studying this CdS functionality we, however, realized that combination of noble metal nanoparticles with CdS/n-TiO_2 combined photocatalyst is not easy to make and gives poor results (cf. also Ref. [12]). Our goal was to synthesize combined photocatalysts by an efficient solution-processed procedure so as to be easy to make and cost effective. Such matters are studied in the present

* Corresponding author. Tel.: +30 2610 997513; fax: +30 2610 997803.
E-mail address: lianos@upatras.gr (P. Lianos).

0920-5861/$ – see front matter © 2010 Elsevier B.V. All rights reserved.
doi:10.1016/j.cattod.2010.03.036

work and a novel design is proposed that leads to efficient hydrogen production.

2. Experimental

2.1. Materials

All materials were from Aldrich unless otherwise specified. Commercial nanocrystalline titania was Degussa P25 and SnO_2:F (FTO) transparent electrodes (resistance 8 Ω/square) were purchased from Hartford, USA.

2.2. Immobilization of n-TiO_2, CdS and Pt on FTO electrodes

Nanocrystalline titania (n-TiO_2) was deposited on FTO electrodes as a paste of commercial Degussa P25 by the following procedure: 10 mL of distilled H_2O was mixed with 10 mL EtOH and 1 g of polyethylene glycol (PEG) 2000. Other PEG sizes may also apply. To this solution we progressively added Degussa P25 under vigorous stirring, followed by sonication. The maximum quantity of titania can vary according to the application. However, for the purposes of the present work it was 2 g. When the mixture was visually a homogeneous solution it was put in a rotary evaporator to evaporate part of the solvent. The obtained paste was at the right viscosity to cast as a thin film on the FTO electrode. For this purpose, FTO transparent electrodes were cut to make orthogonal slides of about 3 cm × 8 cm. They were carefully cleaned by first washing with soap and then sonicating in isopropanol, ethanol and acetone. One part of the slide of dimensions 3 cm × 5 cm (15 cm^2) was then covered by a film of the titania paste. On the rest of the surface of the slide, of dimensions 3 cm × 3 cm (9 cm^2), we applied a solution of about 5 mmol L^{-1} sodium tetrachloroplatinate in ethanol, by taking care not to bring the solution of this salt in contact with the titania-paste film. Ethanol evaporated and left behind a thin film of the dissolved material. Then the FTO slide with the attached films was put in an oven and calcined at 550 °C. Such high temperature was necessary to make sure that all organic content was calcined. The part that supported titania gave a non-transparent white film made of n-TiO_2. The rest of the slide was black due to the deposited Pt. Cadmium sulfide was deposited on the n-TiO_2 film by adsorption of the reagents from aqueous solutions. For this, we first prepared an aqueous solution of 0.1 mol L^{-1} $Cd(NO_3)_2$ and an aqueous solution of 0.1 mol L^{-1} Na_2S. The part of FTO bearing n-TiO_2 was dipped for 5 min in the $Cd(NO_3)_2$ solution, which resulted in adsorption of Cd^{2+} ions by the titania nanocrystalline film. Then the electrode was taken out of the solution, thoroughly washed with water and subsequently dipped in the Na_2S solution for 5 min. During the contact with the sulfur-ion-containing solution, CdS was formed on the titania film. The procedure was repeated 10 times, by taking care to wash with water all excess ions. The deposition of CdS was monitored by reflection–absorption spectrophotometry. Ten dipping procedures were judged sufficient to saturate the titania film with CdS. After formation of CdS, the part of the slide that bore n-TiO_2 was colored yellow. By the above procedure, we obtained FTO electrodes covered by 3/8 of their surface with Pt and by 5/8 of their surface with CdS/n-TiO_2. Of course, other fractions of the surface could be chosen but most of the experiments were performed with this type of surface division. The proposed combination of Pt with semiconductor photocatalyst is equivalent to a photoelectrochemical cell where the anode (i.e., the photocatalyst) is continuously short-circuited with the cathode (i.e., the Pt).

2.3. Reactor design

The reactor was a cylindrical tube, made of Pyrex glass, with one side flattened to let light get in. The height of the solution column was about 10 cm so as to let the FTO slide be completely immersed in the solution. The total quantity of the solution was about 100 mL. The solution was a mixture of EtOH with water and contained also an electrolyte (see below). The upper part of the reactor was closed with appropriate glass fittings having provisions for gas inlet and outlet. All experiments were carried out under constant Ar flow of 20 cm^3/min. Ar was used in order to deaerate the reactor solution and as a carrier gas to carry produced hydrogen to the gas chromatograph. The FTO slide with the deposited active materials was vertically put inside the reactor, just at the position where the reactor was flattened so that the CdS/n-TiO_2 film was fully exposed to the exciting radiation, which was obtained from a xenon source. The intensity of radiation was controlled with multiple wire grids and by the distance between lamp and sample and it was fixed at 100 mW cm^{-2} at the position of the photocatalyst. Monochromatic irradiation was obtained by using interference filters. In that case, the intensity depended on the filter used and it was much weaker (see below).

2.4. Apparatus

Detection of hydrogen was made online by using an SRI 8610C gas chromatograph and Ar as carrier gas. Samples were periodically collected via an automatic gas-sampling valve and the concentration of H_2 present in the reactor effluent was determined as a function of time of irradiation. Calibration of the GC signal was accomplished with the use of a standard mixture of 0.25% H_2 in Ar. Illumination of the samples was made with a 400 W xenon lamp (Oriel). The intensity of radiation at the position of the catalyst was measured with an Oriel Radiant Power Meter. UV–vis absorption measurements were made with a Cary 1E spectrophotometer. Images at various magnifications were recorded with a FESEM (Zeiss SUPRA 35VP; acceleration voltage at 10 kV). X-ray microanalysis measurements were carried out with the aid of QUANTAX 200 model unit (Bruker AXS). The TiKα_1, CdLα_1 and SKα_1 line was used for the concentration profiles. XRD patterns were recorded with a D8 ADVANCE (Bruker AXS) diffractometer working in Bragg–Brentanno θ–θ geometry (source: CuKα, power: 1.6 kW).

3. Results and discussion

Use of n-TiO_2 immobilized on glass slides has been successfully made in previous works [7,8]. The problem arose when we tried to sensitize titania by using a Visible-light-absorbing photosensitizer. As already said, it is difficult to find an organic molecular sensitizer of titania in aqueous environments, even though, there is a rich literature on this matter [13,14]. CdS does act as sensitizer in aqueous environment, however, the efficiency of CdS/n-TiO_2 combined photocatalyst for hydrogen production is very low, practically zero. It was obvious that the presence of an electron sink, i.e., a high work function metal, which collects and traps excited electrons, was necessary. However, when Pt was deposited on CdS/n-TiO_2, it did not work either. Even though, the explanation for this failure is not clear, it seems that the simultaneous presence of CdS and Pt on the surface of n-TiO_2 is not compatible. For this reason, we decided to spatially separate Pt from CdS/n-TiO_2. Subsequently, they were deposited on a transparent conductive electrode, as detailed in the previous section. The conductive substrate was, of course, necessary to provide a channel for draining excited electrons away from the excited photocatalyst. This combination of Pt and CdS/n-TiO_2 on FTO is equivalent to a photoelectrochemical cell with anode (i.e., semiconductor) and cathode (i.e., Pt) always under short-circuit conditions.

The combined CdS/n-TiO_2 photocatalyst was studied by various characterization techniques. The UV–vis absorption spectrum,

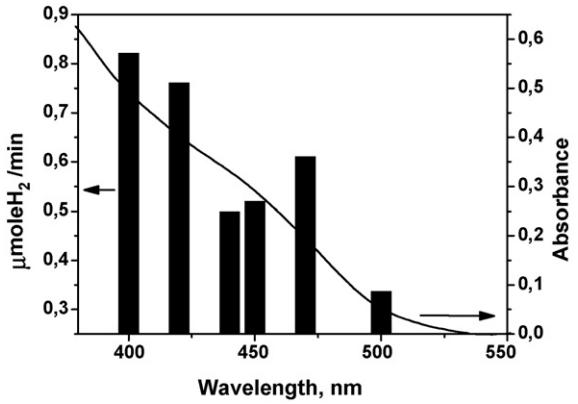

Fig. 1. Absorption spectrum of the CdS/n-TiO_2 photocatalyst and the hydrogen production rate at selected wavelengths within the same spectral region. Bars were recorded with 10% uncertainty.

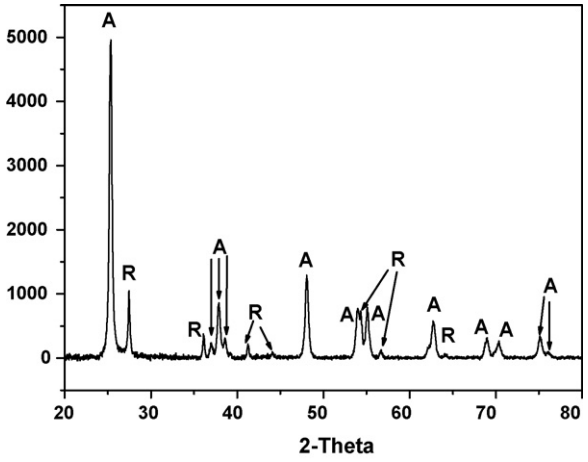

Fig. 2. XRD pattern from the combined CdS/n-TiO_2 film: A, Anatase; R, Rutile.

shown in Fig. 1, possessed the typical absorption features of nanoparticulate CdS, as it is very well known from the rich related literature (cf. Ref. [15]). Comparison with previous data treating CdS/n-TiO_2 photocatalyst [15], shows that the spectrum of Fig. 1 corresponds to a rather small weight percentage of CdS. XRD analysis of the combined photocatalyst gave only the diffraction peaks, which correspond to titania P25, i.e., a mixture of Anatase and Rutile nanocrystals, as can be seen in Fig. 2. No CdS diffraction pattern was detected, indicating that the presently synthesized material is either of poor crystallinity or its weight percentage is too small to be detected.

We have not managed to detect CdS nanoparticles on nanoparticulate titania by microscopy techniques either. TEM images detected only titania nanoparticles and the same was true also for FESEM images. A cross-sectional FESEM view of the CdS/n-TiO_2 film can be seen in Fig. 3a. The thickness of the film was 10 μm.Its nanostructure is distinguished in Fig. 3b. We performed an EDX analysis across the film to detect the distribution of Ti, Cd and S atoms. No variation of atomic distribution was detected with depth, as can be seen in Fig. 3c. This interesting finding suggests that during adsorption, Cd^{2+} and S^{2-} ions penetrate deeply into the TiO_2 mesoporous structure providing an even distribution. Even distribution discourages CdS aggregation, which would have led to cluster formation and easier detection by microscopy. We then conclude that CdS is most probably accommodated within the mesoporous structure of titania and takes the form of very small and evenly distributed nanoparticles.

Spatial separation of the electron sink from the oxidation site, i.e., Pt from the semiconductor nanoparticles, means that it is necessary for the hydrogen ions produced during photooxidation to move substantial distances within the solution. Consequently, the solution must allow for substantial ionic conductivity. For this reason, it was necessary to add an electrolyte. Thus, some experiments were first performed in order to decide, which electrolyte was the best. The effect of various electrolytes on the PC production of hydrogen by using the above described photocatalyst configuration is demonstrated in Fig. 4. The system did not work in the presence of acids. In fact the photocatalyst was detached from the electrode at low pH. The system did work in the presence of a basic electrolyte. The curves of Fig. 4 consist of a rising part, which characterizes the time period of molecular hydrogen accumulation into the reactor tubing, and a plateau, which represents the time period of stable hydrogen production rate. This rate was different when different electrolytes were added in the reactor solution. Absence of any electrolyte gave practically zero hydrogen while for the same quantity of electrolyte (curves 2 and 3) NaOH proved itself much more efficient than Na_2SO_3. Hydrogen production rate was even higher in the presence of 0.2 mol L^{-1} NaOH but decreased for further increase of NaOH concentration. Thus most of the measurements in this work were carried out in the presence of 0.2 mol L^{-1} NaOH. The importance of NaOH indicates that most of the PC process is affected by the presence of OH ions, which, as already said, apparently act as intermediates of the oxidation process. When the hydroxyl concentration became too high, apparently, many photogenerated hydrogen ions interacted with hydroxyl groups producing water. Thus the hydrogen production rate declined at too high NaOH concentration. The data of Fig. 1 were obtained in the presence of 20 vol.%. EtOH. The quantity of EtOH in the reactor solution does play a role, which is analyzed in the following paragraph.

Fig. 5 shows the hydrogen evolution rates in the presence of various quantities of EtOH under white light illumination. EtOH was chosen as a model compound for PC hydrogen production since, as it has been previously found, it fits well the study of such processes [7,8]. In the absence of EtOH, a small quantity of hydrogen was produced, apparently by oxidative water splitting. As the quantity of ethanol increased, so did the hydrogen production rate. The highest in the present work was observed at 50 vol.%. EtOH. It is noted that above 10% EtOH, the increase of the hydrogen production rate with alcohol concentration was small (see further discussion below). It must be also underlined that no oxygen production was detected in any of the measurements of the present work. This was expected, since oxidation of ethanol leads to carbon dioxide and not to O_2 formation [3].

In order to estimate the quantum efficiency of the process and thus judge the photocatalytic capacity of the present photocatalyst, hydrogen production rates were studied as a function of the wavelength of the incident radiation. A series of interference filters were used for this purpose. The intensity of radiation falling on the photocatalyst in each case was measured with a radiant power meter. Fig. 1 shows the absorption spectrum of CdS on titania together with the hydrogen production rate for chosen (filtered) wavelengths. The rates were corrected for the intensity of the radiation passing through the filter. This correction creates an important error (about 10%), particularly at shorter wavelengths, where Xe lamps emit the weakest radiation. Even under these conditions, the trend of the hydrogen production rate follows the photocatalyst light–absorption profile, clearly indicating that the present case is a result of photosensitization by Visible radiation and not, for example, a result of leaking UV radiation. The next step was to study again the effect of EtOH concentration at a chosen wavelength, namely 470 nm. Monochromatic radiation allows proper measurement of the quantum efficiency by the following considerations. A rough

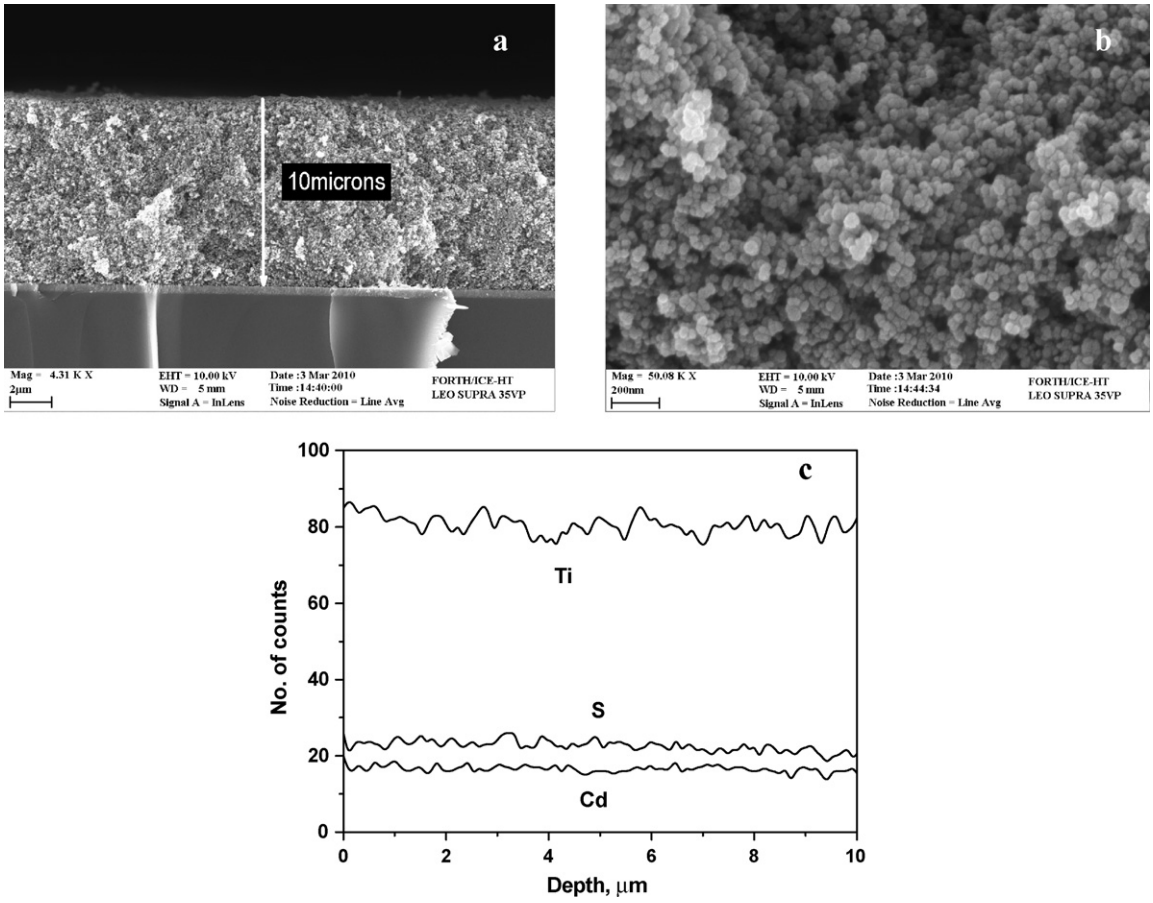

Fig. 3. (a) Cross-sectional profile of the CdS/n-TiO_2 film. (b) Nanostructure of the film. Nanoparticles belong to Degussa P25. (c) Variation of the concentration of Ti, Cd and S as a function of the depth within the film studied by EDX.

estimation of the quantum efficiency can be obtained by calculating the total number of hydrogen molecules produced in the unit of time and the total number of photons incident on the catalyst in the same time. It should be noted that 2 electrons are necessary for production of one hydrogen molecule. Thus for a rate of R (μmol/min), the total number of effective electrons involved per unit of time is $n_e = 2 \times R \times 10^{-6} N/60$ electrons/s, where N is the Avogadro's number. If the corresponding incident radiant power on the catalyst is P (in mW), the number of incident photons per unit of time is $n_p = 10^{-12} \times P \times \lambda/hc$, where λ is the wavelength in nm, h is the Planck's constant, and c is the speed of light. Thus the quantum yield of functional electrons at the specific wavelength λ will be given by $\varphi = n_e/n_p$, i.e.,

$$\varphi = \frac{3988 \times R(\mu\text{mol/min})}{\lambda(\text{nm}) \times P(\text{mW})} \quad (1)$$

The area of the photocatalyst, as already said, was 15 cm^2 while the radiation intensity, filtered at 470 nm, at the position of the photocatalyst was 0.32 mW cm^{-2}. Therefore, in this case $P = 15 \times 0.32 = 4.8$ mW. By introducing this value of P and the value of the corresponding R (listed in Table 1) we obtained the values of φ, also listed in Table 1. The values of the hydrogen production rates of the second column of Table 1 are also plotted in Fig. 6. It is noted that after a fast increase of hydrogen production rate up to 10% EtOH, further increase of EtOH, gave a small further increase of hydrogen production rate. 50 vol.% EtOH gave the high-

Table 1
Values of the hydrogen production rate and quantum efficiency for functional electrons generation under monochromatic radiation (470 nm). The reactor solution contained 0.2 mol L^{-1} NaOH and various ethanol–water mixtures. Incident light intensity was 0.32 mW cm^{-2}.

Volume percentage of EtOH	H_2 production rate (μmol/min)	Functional electrons yield φ (%)
2	0.07	12
5	0.12	21
10	0.16	29
20	0.19	34
50	0.21	37
80	0.17	30

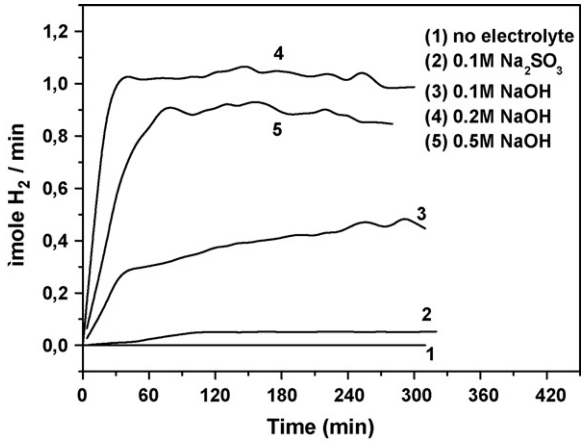

Fig. 4. Variation of the quantity of molecular hydrogen produced in the presence of different electrolytes. The electrolyte solution in all cases contained 20 vol.% EtOH.

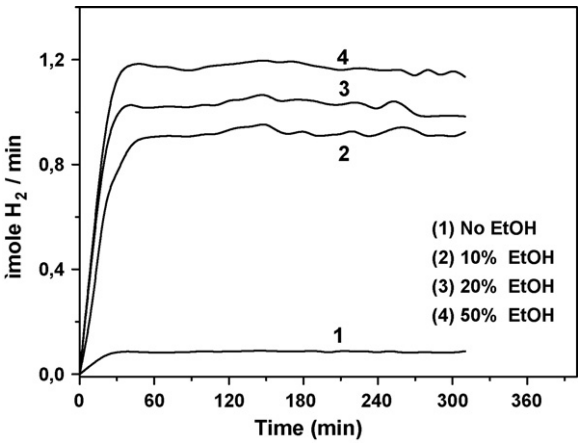

Fig. 5. Variation of the quantity of molecular hydrogen produced in the presence of various quantities of ethanol and 0.2 mol L^{-1} NaOH.

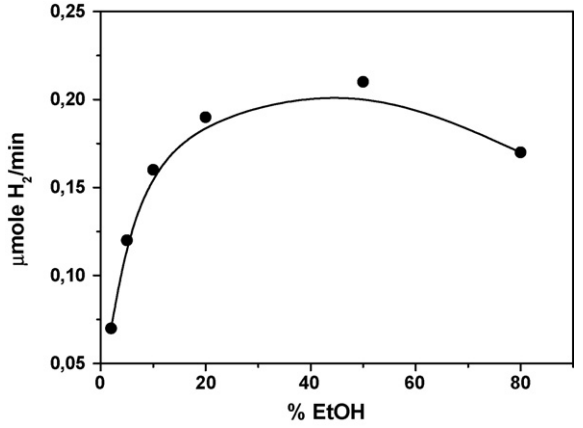

Fig. 6. Variation of the quantity of molecular hydrogen produced in the presence of various quantities of ethanol and 0.2 mol L^{-1} NaOH under 470 nm monochromatic irradiation.

est rate. Further increase had adverse effects. As expected, the yield of functional electrons varied accordingly. The maximum yield was 37% and it was obtained in the presence of 50 vol.% EtOH. These values are very good but we believe that higher values might be accessible. For this purpose, further work is under course in our laboratory.

4. Conclusions

Spatial separation of the reduction catalyst Pt from the combined CdS/n-TiO_2 photocatalyst by using a FTO slide allowed functioning of the photocatalyst under Visible irradiation and led to photocatalytic hydrogen production. Hydrogen was produced also by using pure water and a NaOH electrolyte but in the presence of ethanol, hydrogen evolution rate was almost 10 times higher.

Acknowledgements

Financial support from E.ON International Research Initiative is gratefully acknowledged. Responsibility for the content of this publication lies with the authors.

References

[1] T. Sakata, T. Kawai, Chem. Phys. Lett. 80 (1981) 341.
[2] M. Kaneko, J. Nemoto, H. Ueno, N. Gokan, K. Ohnuki, M. Horikawa, R. Saito, T. Shibata, Electrochem. Commun. 8 (2006) 336.
[3] D.I. Kondarides, V.M. Daskalaki, A. Patsoura, X.E. Verykios, Catal. Lett. 122 (2008) 26.
[4] A. Galinska, J. Walendziewski, Energy Fuels 19 (2005) 1143.
[5] Y. Mizukoshi, Y. Makishe, T. Shuto, J. Hu, A. Tominaga, S. Shironita, S. Tanabe, Ultrason. Sonochem. 14 (2007) 387.
[6] N. Strataki, N. Boukos, F. Paloukis, S.G. Neophytides, P. Lianos, Photochem. Photobiol. Sci. 8 (2009) 639.
[7] N. Strataki, V. Bekiari, D.I. Kondarides, P. Lianos, Appl. Catal. B 77 (2007) 184.
[8] N. Strataki, P. Lianos, J. Adv. Oxid. Technol. 11 (2008) 111.
[9] M. Ashokkumar, Int. J. Hydrogen Energy 23 (1998) 427.
[10] M. Sathish, R.P. Viswanath, Catal. Today 129 (2007) 421.
[11] M. Antoniadou, P. Lianos, J. Photochem. Photobiol. A 204 (2009) 69.
[12] A. Sobczynski, A.J. Bard, A. Campion, M.A. Fox, T. Mallouk, S.E. Webber, J.M. White, J. Phys. Chem. 91 (1987) 3316.
[13] M. Ni, M.K.H. Leung, D.Y.C. Leung, K. Sumathy, Renew. Sustain. Energy Rev. 11 (2007) 401.
[14] D. Chatterjee, Catal. Commun. 11 (2010) 336.
[15] L. Wu, J.C. Yu, X. Fu, J. Mol. Catal. A: Chem. 244 (2006) 25.